

Urban Heat Island Amplification Estimates on Global Warming Using an Albedo Model

Alec Feinberg

Key Words: Urban Heat Islands, Albedo Modeling, UHI Amplification Effects, Global Warming Causes And Amplification Effects, UHI Footprint, UHI Heat Dome, Cool Roofs, Sea Ice, and Water Vapor Feedbacks

Abstract In this paper, we provide nominal and worst-case estimates of radiative forcing due to UHI effect using a Weighted Amplification Albedo Solar Urbanization (WAASU) model. This is done with reported findings from UHI footprint and heat dome studies that simplify estimates for UHI amplification factors. Using this method, we are able to quantify a global warming range due to the UHI effect (including urban area). Variations in our estimates are due to urbanized area assessments and amplification factor uncertainties. However, the model showed consistent estimates of about 0.096W/m^2 per % Normalized Effective Amplified Area for the urbanized area feedback value. These values increase when the UHI root-cause assessment of its contribution to climate feedback problems is evaluated. The model is additionally used to quantify a warming assessment due to sea ice feedback. Results provide insight into the UHI area effects from a new perspective and illustrates that one needs to take effective UHI amplification factors into account when assessing UHI's warming effect on a global scale. Lastly, such effects likely show a persuasive argument for the need of world-wide UHI albedo goals.

1 Introduction

There are few recent publications about possible UHI influences on global warming. Part of this paper's motivation is to illustrate the continual need for more up-to-date related studies, including UHI amplification effects that will be discussed in this paper. The subject of UHI effect having significant contributions to global warming is critical and should remain so. The topic has a controversial history. One such paper, by McKittrick and Michaels (2007), found that the net warming bias at the global level may explain as much as half the observed land-based warming. This study was criticized by Schmidt (2009) and defended by Mckitrick (see McKittrick Website) over many years. Other authors have also found significance (Zhao, 1991; Feddema et al., 2005; Ren et al., 2007, 2008; Jones et al., 2008; Stone, 2009; Zhao, 2011; Yang et al. 2011, and Haung et al. 2015). These studies used land-based temperature station data to make assessments. In our study, where we introduce a Weighted Amplification Albedo Solar Urbanization (WAASU) model, we will see it has some advantages over these ground-based temperature studies. The model is non-probabilistic, in line with the way typical energy budgets are calculated. It uses only two key parameters: normalized effective amplified area and average albedo. Because it is simplistic, it has transparency compared with the complex land-based studies.

The contention that UHI effects are basically only of local significance is most likely related to urban area estimates. For example, the IPCC (Satterthwaite et. al. 2014) AR5 report references a Schneider et al. (2009) study that resulted in urban coverage of 0.148% of the Earth (Table 1). This seemingly small area tends to dismiss the contention that the UHI effect can play a large-scale role in global warming. Furthermore, estimates of how much of land has been urbanized vary widely in the literature, in part due to the definition of what is urban and the datasets used. Although, such estimates are important for environmental studies, obtaining true estimates for the small urbanized area relative to the total land is apparently very difficult. Compounded by the fact that there is a significant difference in how groups define the term "urban". Urbanized surface area land approximations vary widely, and most are obtained with satellite measurements sometimes supplemented with census data. Table 1 captures the variations from select papers of interest.

In addition, global warming UHI amplification effects have not been quantified to a large degree related to area estimates. Urbanized average solar areas remain unknown.

Table 1. Urbanization area extent estimates from various sources

Percent of Land	Percent of Earth	References
2.7	0.783	GRUMP, 2005 – using NASA satellite light studies based on 2004 data and supplemented with census data
1	0.29	NASA, 2000; Galka, 2016 – from satellite data
0.51	0.148	Schneider et al. 2009 – based on 2000-2001 data and referenced in the IPCC report (Satterthwaite, 2014)
0.5	0.145	Zhou 2015 – based on a 2000 data set

56
57
58
59
60
61
62
63
64
65
66
67
68
69
70
71
72

In our study, one key paper listed in Table 1 is due to Schneider et al. (2009) since it is cited by the AR5 2014 IPCC report (Satterthwaite et al. 2014). In Schneider's paper, the larger area found in the GRUMP 2005 study (Table 1) is criticized. These area estimates are of interest in our paper for the WAASU model. Additionally, the amplification factors we use are related to their urban coverage estimates. In this paper we use both the Schneider et al. and GRUMP studies for the nominal and worst cases urbanization area estimates respectively. Furthermore, they were both done using data sets near the year 2000, a good point in time to extrapolate down to 1950 and up to 2019 (see Sec. 3).

1.1 UHI Amplification Effects

The table below lists global warming causes and amplification effects. In this section we will summarize only the UHI amplification effects listed in the table since the root causes and the main global warming feedback amplification effects are fairly well known.

Table 2. Global warming cause and effects

Global Warming Causes →	Population → Expanding Urban Heat Islands (UHI), Roads & Increases in Greenhouse Gas
Global Warming Feedback Amplification Effects →	Water Vapor Feedback, Land Albedo Change Due to Cities & Roads, Ice and Snow –Albedo Feedback, Lapse Rate Feedback, Cloud Feedback, etc.
Urban Heat Island Amplification Effects →	UHI Solar Heating Area (Building Areas), UHI Building Heat Capacities, Humidity Effects and Hydro-Hotspots, Reduced Wind Cooling, Solar Canyons, Loss of Wetlands, Increase in Impermeable Surfaces, Loss of Evapotranspiration Natural Cooling.

73
74
75
76
77
78
79
80
81
82
83
84
85
86
87
88
89
90
91
92
93
94
95
96
97
98

The UHI amplification effects that we consider to dominate listed in the table are as follows:

- **The humidity amplification effect:** This effect has been observed. For example, Zhao et al. (2014) noted that UHI temperature increases in daytime ΔT by 3.0°C in humid climates but decreasing ΔT by 1.5°C in dry climates. They noted that such relationships imply UHIs will exacerbate heat wave stress on human health in wet UHI climates. One explanation is how heat dissipates through convection which is more difficult in humid climates. Another explanation is that warmer air holds more water vapor. This can increase local specific humidity so that there could be local greenhouse effects.
- **The heat capacity and solar heating area amplification effect:** This effect contributes to the day-night UHI cycle. In most cities, it is observed that daytime atmospheric temperatures are actually cooler compared to night. For example, in a study by Basara et al. (2008) in Oklahoma city UHI, it was found that at just 9-m height, the UHI was consistently $0.5\text{--}1.75^{\circ}\text{C}$ greater in the urban core than the surrounding rural locations at night. Further, in general UHI impact was strongest during the overnight hours and weakest during the day. This inversion effect can be the result of massive UHI buildings acting like heat sinks, having giant heat capacities and storing heat in their reservoir via convection as solar radiation is absorbed during the day. This occurrence often reduces the UHI day effect, but at night buildings cool down, giving off their stored heat that increases local temperatures to the surrounding atmosphere. This effect increases with city growth as buildings have gotten substantially taller since 1950 (Barr 2019).
- **The hydro-hotspot amplification effect:** This effect is not well addressed. Atmospheric moisture source is a complex issue due to Hydro-HotSpots (HHS). HHS occurs when buildings are hot due to sun exposure. Then, during precipitation periods, the hot evaporation surfaces increase localized water vapor as warm air holds more moisture. This increase in local greenhouse gas could blanket city heat and increase infrared radiation during these periods, providing another UHI humidity amplification source.
- **Reduced wind cooling and solar canyons:** In UHIs reduced wind is a known effect due to building wind friction, that inhibits cooling by convection. Tall buildings also create solar canyons and trap sunlight, reducing the average albedo, although some benefits occur from shading. In general, both have the effect of amplifying the temperature profile of UHIs.

100
101
102
103
104
105
106
107
108

2 Data and Methods

We see from the previous section that estimating climate change impact just based on the UHI area coverage as in Table 1, does not take into account of the effects of solar heating building sidewall areas, massive heat capacities,

109 humidity issues, wind reduction and the solar canyon trapping that collectively amplify UHI effects beyond its own
110 climate area.

111 **2.1 UHI Area Amplification Factor**

112
113 To estimate the UHI amplification effects, it is logical to first look at UHI footprint (FP) studies as they provide
114 some measurement information. Zhang et al. (2004) found the ecological FP of urban land cover extends beyond the
115 perimeter of urban areas, and the FP of urban climates on vegetation phenology they found was 2.4 times the size of
116 the actual urban land cover. In a more recent study by Zhou et al. (2015), they looked at day-night cycles using
117 temperature difference measurements in China. In this study, they found UHI effect decayed exponentially toward
118 rural areas for the majority of the 32 Chinese cities. Their comprehensive study spanned from 2003 to 2012. They
119 describe China as an ideal area to study since it has experienced the most rapid urbanization in the world in the
120 decade they evaluated. They found that the FP of UHI effect, including urban areas, was 2.3 and 3.9 times that of
121 urban size for the day and night, respectively. We note that the average day-night amplification footprint coverage
122 factor is 3.1.

123 Looking at Table 2, we see that the UHI Amplification Factor (AF) is highly complex making it difficult to assess
124 from first principles as it would be some function of Table 2 components relative to a reference year:

$$125 \quad AF_{UHI \text{ for } 2019} = f\left(\overline{Build}_{Area} \times \overline{Build}_{C_p} \times \overline{R}_{wind} \times \overline{LossE}_{vtr} \times \overline{Hy} \times \overline{S}_{canyon}\right) \quad (1)$$

126 were

127 \overline{Build}_{Area} = Average building solar area

128 \overline{Build}_{C_p} = Average building heat capacity

129 \overline{R}_{wind} = Average city wind resistance

130 \overline{LossE}_{vtr} = Average loss of evapotranspiration to natural cooling & loss of wetland

131 \overline{Hy} = Average humidity effect due to hydro-hotspot

132 \overline{S}_{canyon} = Average solar canyon effect

133
134 To provide some estimate of this factor, we note that Zhou et al. (2015) found the FP physical area (km²), correlated
135 tightly and positively with actual urban size having a correlation coefficients higher than 79%. This correlation can
136 be used to provide an initial estimate of this complex factor. Therefore, as a model assumption, it seems reasonable
137 to use area ratios for this estimate.

$$138 \quad AF_{UHI \text{ for } 2019} = \frac{\sum(UHI \text{ Area})_{2019}}{UHI \text{ Area}_{1950}} \quad (3)$$

139 Area estimates have been obtained in the next Section in Table 3 between 2019 and 1950 time frames, yielding the
140 following results for the Schneider et al. (2009) and the GRUMP (2005) extrapolated area results:

$$141 \quad AF_{UHI \text{ for } 2019} = \frac{(Urban \text{ Size})_{2019}}{(Urban \text{ Size})_{1950}} \approx \begin{cases} \left(\frac{[0.188]_{2019}}{[0.059]_{1950}} \right)_{Schneider} & = 3.19 \\ \left(\frac{[0.952]_{2019}}{[0.316]_{1950}} \right)_{GRUMP} & = 3.0 \end{cases} \quad (3)$$

142 Between the two studies, the UHI area amplification factor average is 3.1. Coincidentally, this factor is the same
143 observed in the Zhou et al. (2015) study for the average footprint. This factor may seem high. However, it is likely
144 conservative as other effects would be difficult to assess: increases in global drought due to loss of wet-lands,
145 deforestation effects due to urbanization, and drought related fires. It could also be important to factor in changes of
146 other impermeable surfaces since 1950, such as highways, parking lots, event centers, and so forth.

147
148 The area amplification value of 3.1 is then considered as one of our model assumptions.

149
150
151

152 **2.2 Alternate Method Using the UHI's Dome Extent**

153

154 An alternate approach to check the estimate of Equation 3, is to look at the UHI's dome extent. Fan et al. (2017)
 155 using an energy balance model to obtain the maximum horizontal extent of a UHI heat dome in numerous urban
 156 areas found the nighttime extent of 1.5 to 3.5 times the diameter of the city's urban area (2.5 average) and the
 157 daytime value of 2.0 to 3.3 (2.65 average).

158

159 Applying this energy method (instead of the area ratio factor in Eq. 3), yields a diameter in 2019 compared to that of
 160 1950 with an increase of 1.8. This method implies a factor of $2.5 \times 1.8 = 4.5$ higher in the night and $2.65 \times 1.8 = 4.8$ in
 161 the day in 1950 with an average 4.65. This increase occurs 62.5% of the time according to Fan et al., where their
 162 steady state occurred about 4 hours after sunrise and 5 hours after sunset yielding an effective UHI amplification
 163 factor of 2.9. We note this amplification factor is in good agreement with Equation 3. Fan et al. assessed the heat
 164 flux over the urban area extent to its neighboring rural area where the air is transported from the urban heat dome
 165 flow. Therefore the heat dome extends in a similar manner as observed in the footprint studies. If we use the dome
 166 concept, we can make an assumption that the actual surface area for the heat flux is increased by the surface area of
 167 the dome. We actually do not know the true diameter of the dome, but it is larger than the assessment by Fan et al..
 168 Using the dome extend due to Fan et al. applied to the area of diameter D , the amplification factor should be
 169 correlated to the ratios of the dome surface areas:

170

$$171 \quad AF_{UHI \text{ for } 2019} = \left(\frac{D_{2019}}{D_{1950}} \right)^2 = 2.9^2 = 8.4 \quad (4)$$

172 Thus, this equation is our second model assumption, where it is reasonable to use the ratios of the dome's surface
 173 area for an alternate approach in estimating the effective UHI amplification factor. We will have two values, 3.1 and
 174 8.4, to work with which will help in assessing model consistency and provide upper and lower bounds for effective
 175 area amplification which must occur based on these authors' observations and the dependence in Equation 1.

176

177 **2.3 Applying the Amplification Factors**

178

179 In this analysis, 1950 is the reference year. Therefore it is not subjected to amplification. Only the new area is
 180 amplified as we are looking at changes since this time frame. This is denoted as the Amplified Effected Area (AEA).
 181 The AEF in 2019 is then given by

182

$$183 \quad AEA_{UHI \text{ for } 2019} = AF(\text{newarea}) + Area_{1950} = AF(Area_{2019} - Area_{1950}) + Area_{1950} \quad (5)$$

184 Using this, if there were no changes in UHI growth, for example so that the $Area_{2019} = Area_{1950}$, the resulting area is
 185 just the original $Area_{1950}$. This result is applied to the new area in Table 3 below.

186

187 **2.4 Area Extrapolations for 1950 and 2019**

188

189 To assess the urbanized area, (also used in determining the UHI amplification factor ratios above), we need to
 190 project the Schneider and GRUMP area estimates down to 1950 and up to 2019. Both use datasets are near to 2000,
 191 so this is a convenient somewhat middle time-frame. Here we decided to use the world population growth rate
 192 (World Bank 2018) which varies by year as shown in Appendix A in Figure A1. We used the average growth rate
 193 per $\frac{1}{2}$ decade for iterative projections of about 1.3% to 1.6% per year.

194

195 To justify this projection, we see that Figure A2a illustrates that building material aggregates (USGS 1900-2006)
 196 used to build cities and roads correlates well to population growth (US Population Growth 1900-2006).

197

198 It is also interesting to note that building materials for cities and roads also correlates well to global warming trends
 199 (NASA 1900-2006) shown in Figure A2b.

200

201 Column 2 in Table 3 show the projections with the actual year (~2000) data point tabulated value also listed in the
 202 table (see also Table 1). The UHI area amplification factor of 3.1 (Column 3) is then applied to Schneider and
 203 GRUMP studies shown in Column 4 using Equation 5.

204

205

206

207

208

Table 3. Extrapolated and amplified urbanized coverage estimates

Year	Urban coverage percent of Earth	Amplification factor effect	Amplification Effected Area (AEA)
Schneider study			
1950	0.059*	1	0.059%
2000-2001	0.0051x29%=0.148		
2019	0.188*	3.1 AF _{Area} **	0.459%
2019	0.188*	8.4 AF _{Dome} **	1.143%
Worst case GRUMP study			
1950	0.316%*	1	0.316%
2000	0.027x29%=0.783%		
2019	0.952%*	3.1 AF _{UHI} **	2.288%
2019	0.952%*	8.4 AF _{Dome} **	5.658%

*Growth rate of cities using world population yearly growth rate in Fig A1, **AF_{UHI} is the area amplification factor for 2019 referenced to 1950.

209

210

211

212 **2.5 Weighted Amplification Albedo Solar Urbanization (WAASU) Model Overview**

213

214 The WAASU model is very straightforward; it is based on a global weighted albedo model. The Earth Albedo is
215 given by

$$216 \quad \text{Earth Albedo} = \sum_i \{ \% \text{Effective Surface Area}_i \times \text{Surface Item Albedo}_i \} + \text{Cloud Area} \times \text{Cloud Albedo}. \quad (6)$$

217 Here the effective surface area is given by

218

$$219 \quad \text{Effective Surface Area} = \text{Surface Area} \times \% \text{Solar Irradiance}. \quad (7)$$

220

221 where the surface area includes all areas including AEA. We note that the change in the Earth Albedo change over
222 time (from 1950 to 2019), is just a function of the UHI area variation, (when holding all unrelated UHI components
223 fixed), that is

$$224 \quad \left(\frac{dEA}{dt} \right)_{EA'} = \sum_i \left(\text{Albedo}_{UHI} \times \text{Solar Irradiance} \times \frac{d\text{Area}_{UHI}}{dt} \right)_i, \quad (8)$$

225

226 where EA is the Earth's albedo, and EA' is all other Earth components (held fixed). Although it is possible that the
227 solar irradiance percent changes due to new city locations, in this model we assume it is fixed at 100%. This
228 indicates, for example, that even if we were to change the *Effective Surface Area* of perhaps the *sea ice component*
229 because it receives about 40% irradiance compared with other areas and redistributed its radiance (per the Earth's
230 energy budget), it would not affect the overall results when looking at the albedo change due to the UHI effect from
231 1950 to 2019. Therefore, the model only requires we work with normalized area coverage changes when focusing
232 solely on the UHI effect. On the other hand, solar irradiance comes into play for sea ice when we are considering its
233 global albedo effect from 1950 to 2019 (see Appendix C). However, the solar radiation weighting, albedo, and areas
234 for all Earth components are subjected to the constraints below.

235

236 **2.5.1 Model Constraints**

237

238 This model is subject to the constraint

$$239 \quad \text{Total Area} = \sum_i \{ \% \text{Normalized Effective Amplified Surface Areas}_i \} + \% \text{Cloud Area} = 100\% \quad (9)$$

240

241 and the normalization effective amplified area (NEAA) constraint for the Earth surface areas (when the UHI area is
242 increased) must then be subject to

243

$$244 \quad \sum_i \{ \% \text{Normalized Effective Amplified Surface Areas}_i \} = 100\% - \% \text{Cloud Area}. \quad (10)$$

245
246
247
248
249
250
251
252

To simplify things as much as possible, **only five Earth constituents are used:** *water, sea ice, land, UHI coverage, and clouds* (where *land* is its area minus the UHI coverage). These components are fairly easy to estimate and references for their values are provided in Appendix D. Furthermore, we use consistent values found in the IPCC AR5 report (Hartmann et al., 2013) assessment of the Earth's energy budget for solar irradiance. Table 4 summarizes the constraints from these IPCC values.

253 The fixed components of our model maintain relative consistency from 1950 to 2019. The non-fixed value is the urban coverage as indicated by Equation 8. The only unknown value is the *land* albedo (minus the UHI coverage) and this value is adjusted to obtain the IPCC global albedo of 29.4118% and its *land* value of incident/reflected value of 7.0588.

Table 4. IPCC Earth energy budget values (Hartmann et al., 2013)

IPCC Item	Incident and Reflected Radiation (W/m ²)	Albedo %	Absorbed (W/m ²)
Earth	100/340	29.4118	240=340x(1-.294)
Atmosphere & Clouds	76/340	22.3529	79
Earth Surface Albedo	24/340	7.0588	161

258 These values are used as a 1950 starting point and then the 2019 increase for UHI coverage area is inserted. This increases the Earth's area to greater than 100%. Therefore, renormalization is done per the constraint of Equation 10 (detailed in Appendix B).

262 263 3 Results and discussion

264 Using the extrapolated area coverage in Table 3 with the 3.1 amplification factor applied to the urbanized growth, the resulting global albedo change occurred of 29.3956% in 2019 (Table 5b) compared to the earlier 1950 albedo value of 29.4118% (Table 5a) for the Schneider nominal case. As well, for the GRUMP worst case, the albedo changed from 29.4118% (Table 6a) to 29.3322% (Table 6b) due to the urbanized growth.

269 As we mentioned earlier, the increases in the solar surface area of the Earth, which will occur with city growth of tall buildings and their solar areas, however comparatively small, requires renormalization in the model of the Earth surface components of the WAASU model (detailed in Appendix B). This information is displayed in Column 3 in Tables 5b and 6b. While the model is sensitive to urban coverage changes, it works well with renormalization showing a high level of consistency to urban coverage proportionality changes. This point is indicated in Table 7 where we find the GRUMP 2019 area feedback is 0.0944% (W/m²)/Norm Area (=0.271/2.87) compared with the Schneider area feedback of 0.0948 (W/m²)/ %Norm Area (=0.055/0.58).

277 Table 7 provides a summary of albedo changes found in the WASSU model along with the expected solar long wave radiation increase. From the above global WAASU model, the estimates of the Earth's radiated long wavelength emissions are set equal to the short wave radiation absorption:

$$281 \quad 282 \quad P_{\text{Total}} = 340 \text{ W/m}^2 (1 - \text{Albedo}). \quad (11)$$

283 Then the change from 1950 to 2019 represents the equivalent increase in long wave radiation is given by

$$284 \quad 285 \quad \Delta P_{\text{Total}} = 340 \text{ W/m}^2 \{ (1 - \text{Albedo})_{2019} - (1 - \text{Albedo})_{1950} \}. \quad (12)$$

286
287
288
289
290
291
292
293
294
295
296

297
298
299

Table 5a. Schneider results (Albedo=29.4118, 1950) **Table 5b.** Schneider results (Albedo=29.3956%, 2019)

Surface	Albedo	% Area of Surface	Normalized Earth Area	Weighted Albedo %
	A	B	C=A x B x (1-0.67)	A x C
Sum of Water Type		71		
Sea Ice	0.6	15	4.95	2.970
Water	0.06	56	18.48	1.109
Sum of Land Type		29		
Land - (UHI + Coverage)	0.3118	28.941	9.55053	2.978
UHI + Coverage	0.12	0.059	0.01947	0.002
		Σ=100.000	33.000	7.05882
			Cloud Area	
Clouds	0.3336	67	67	22.35294
Σ Sum Earth %			100.000	
Σ Global Albedo				29.4118

Surface	Albedo	Normalized % Surface Area	Normalized Earth Area	Weighted Albedo %
	A	B	C=A x B x (1-0.67)	A x C
Sum of Water Type		70.717		
Sea Ice	0.6	14.94	4.9302	2.958
Water	0.06	55.777	18.406	1.1044
Sum of Land Type		29.283		
Land - (UHI + Coverage)	0.3118	28.826	9.513	2.966
UHI + Coverage	0.12	0.4571	0.1508	0.0181
		Σ=100.000	33.000	7.0283
			Cloud Area	
Clouds	0.3336	67	67	22.3530
Σ Sum Earth %			100.000	
Σ Global Albedo				29.3994

300
301

Table 6a. GRUMP results (Albedo=29.4118, 1950) **Table 6b.** GRUMP results (Albedo=29.3322%, 2019)

Surface	Albedo	% Surface Area	Normalized Earth Area	Weighted Albedo %
	A	B	C=A x B x (1-0.67)	A x C
Sum of Water Type		71		
Sea Ice	0.6	15	4.95	2.970
Water	0.06	56	18.48	1.109
Sum of Land Type		29		
Land - (UHI + Coverage)	0.3135	28.684	9.46572	2.968
UHI + Coverage	0.12	0.316	0.10428	0.013
Sum Surface %		Σ=100.000	33.000	7.0588
			Cloud Area	
Clouds	0.3336	67	67	22.3529
Σ Sum Earth %			100.000	
Σ Global Albedo				29.4118

Surface	Albedo	Normalized % Surface Area	Normalized Earth Area	Weighted Albedo %
	A	B	C=A x B x (1-0.67)	A x C
Sum of Water Type		69.627		
Sea Ice	0.6	14.71	4.8543	2.913
Water	0.06	54.917	18.12261	1.087
Sum of Land Type		30.3727		
Land - (UHI + Coverage)	0.3135	28.129	9.28257	2.910
UHI + Coverage	0.12	2.2437	0.740421	0.089
Sum Earth %		Σ=100.000	33.000	6.9100
			Cloud Area	
Clouds	0.3336	67	67	22.3530
Σ Sum Earth %			100.000	
Σ Global Albedo				29.3519

302
303
304
305
306

Results are compiled in Table 7. The table also includes “what if” estimates, if we could change urbanization to be more reflective with cool roofs to reverse the effect.

The overall results are summarized:

- Nominal Schneider case from 1950 to 2019 is 0.042W/m² and 0.113W/m² due to urban area and dome amplification coverage respectively. These figures equate to about 1.18% and 3.2% of global warming assuming the total increase from 1950 is about 0.95°C in 2019.
- Worst GRUMP case from 1950 to 2019 is 0.204W/m² and 0.537W/m² due to urban area and dome amplification coverage respectively. This roughly equates to 5.7 and 15% of global warming assuming the total increase from 1950 is about 0.95°C in 2019.
- We note the consistency of the area feedback parameter having quite small variability and averaging about 0.096 W/m² / %Normalized Effective Amplified Area (%NEAA) and an average albedo feedback value of 3.4 W/m²/Global Albedo change.
- “What if” corrective action results of cool roofs indicates that changing city albedos in both the Schneider and the GRUMP case from 0.12 to an average value of 0.205 would reverse the increase in emission back to 1950 levels.

307
308
309
310
311
312
313
314
315
316
317
318
319
320
321
322
323
324
325
326

Although global warming assessment obtained in the WAASU model, especially for the Schneider case does not appear to show much contribution to global warming, we find that climate feedback estimates increase the estimated root-cause proportion significantly. Examples are provide in Appendix C that help to demonstrate how the root-cause global warming contribution can be as high as 7.3% for the Schneider case and 27% for the GRUMP case (see Table C2).

327
328
329

Table 7. Albedo and radiative increase model results with UHI effective area.

Year	Urban Extent Global Area %	UHI AEA % Area	UHI Normalized EAA Global Surface %Area	Albedo Cities	Global Weighted Albedo	ΔP_{Total} UHI Radiative Increase W/m^2 (%GW)*	Area Feedback
							$\frac{\Delta P_{Total} (W/m^2)}{\%NEAA}$ $\left(\frac{\Delta P_{Total} (W/m^2)}{\Delta Global Albedo} \right)$
Nominal Case Schneider Study							
1950	0.059	0.059	0.059	0.12	29.4118	0	—
2019	0.188	0.459 (Area AF)	0.457	0.12	29.3994	0.0422 (1.18%)*	0.092 (3.4)
2019	0.188	1.143 (Dome AF)	1.1307	0.12	29.3786	0.1129 (3.16%)*	0.1 (3.23)
What if	0.188	0.459, 1.58 (Area-Dome AF)	0.457, 1.13	0.202, 0.209	29.4118	-0.042 -1.129,	—
Worst Case GRUMP Study							
1950	0.316%	0.316	0.316	0.12	29.4118	0	—
2019	0.952%	2.288 (Area AF)	2.2437	0.12	29.3519	0.204 (5.7%)*	0.091 (3.4)
2019	0.952%	5.658 (Dome AF)	5.395	0.12	29.2539	0.537 (15%)*	0.1 (3.4)
What if	0.952%	2.288 5.658	2.2437 5.395	0.2009, 0.2087	29.4118	-0.204 -0.537	—

330
331
332
333

*Percent of Warming estimate, $P=340 \times (1-\text{Albedo})$, $\%GW=\{(P/\epsilon\sigma)^{0.25}_{2019}- (P/\epsilon\sigma)^{0.25}_{1950}\}/0.95^\circ\text{C}$, $\epsilon=1$

4 Conclusions

334
335
336
337
338
339
340
341
342
343
344

In this paper, we were able to provide estimates of UHI effect (with urban areas) on global warming. This calculation was done with the aid of assumptions for area UHI amplification factors. These estimates inserted into our WAASU model found that between 0.042W/m² and 0.537W/m² of radiative forcing is possible according the WAASU model (this result indicates that about 1.2% and 15% of global warming may be due to the UHI effect (with urban areas). This wide variation is due to both the amplification and urban area uncertainties. However, the model found that the effective UHI area feedback estimates were consistent and about 0.096W/m² per %Normalized Effective Amplified Area. Examples are provided in Appendix C to illustrate how the UHI root-cause assessment contributions can increase significantly when its effect on climate feedback problems is considered. The strength of the model is also demonstrated in Appendix C as estimates were obtained for global warming to the loss of sea ice in the last two decades. The final results were very dependent on area estimates and UHI amplification factors, therefore, refined values of both would be important for further study.

345
346

Below we provide suggestions and corrective actions which include:

347
348
349
350
351
352
353
354

- World leaders and IPCC consider providing albedo guidelines for both UHIs and roads similar to the on-going CO₂ efforts.
- Guidelines for future albedo design requirements of cities and roads.
- Recommend an agency like NASA to be tasked with finding applicable solutions to cool down UHIs.
- Recommendation for cars to be more reflective. Although world-wide vehicles likely do not embody much of the Earth’s area, recommending that all new manufactured cars be higher in reflectivity (e.g., silver or white) would help raise awareness of this issue similar to electric automobiles that help improve CO₂ emissions.

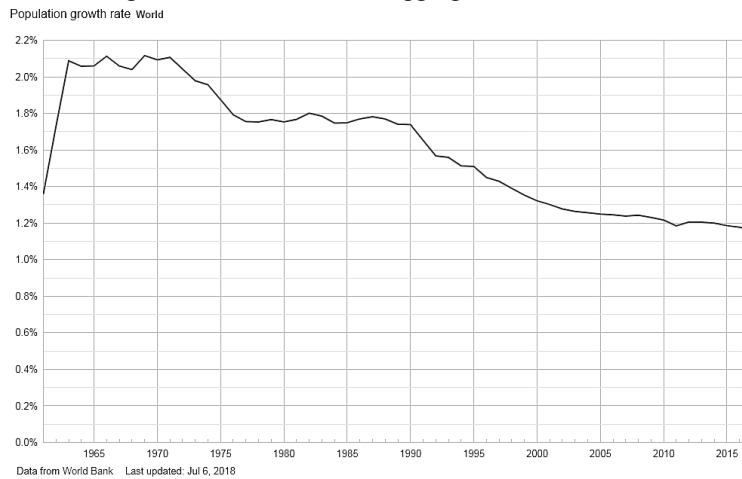
355
356
357

Appendix A: Growth Rates and Information on Natural Aggregates

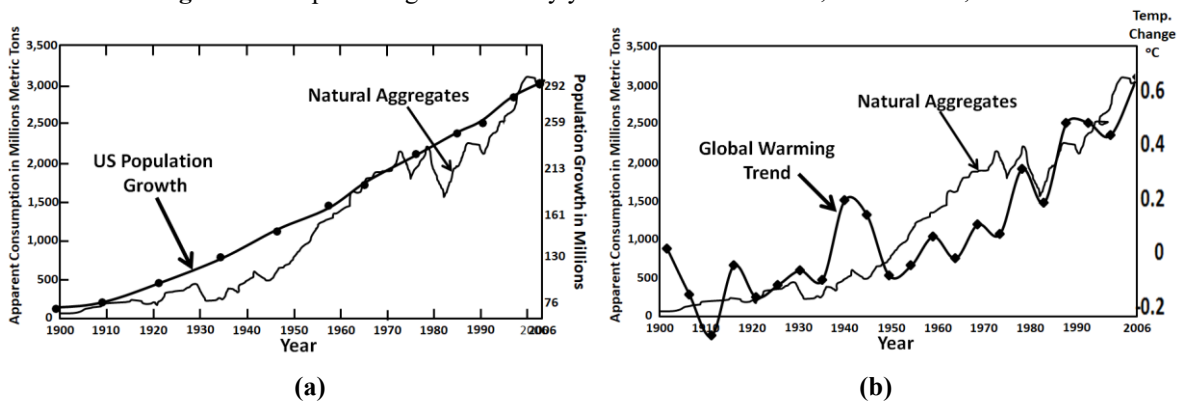
358
359

Below is a plot of the world population growth rate that varies from about 2.1 to 1.1. This graph is used to make growth rate estimates of urban coverage. We note that natural aggregates used to build cities and roads are

360 reasonably correlated to population growth in Figure A2a. Also of interest (Fig. A2b) is the fact that one can see
 361 some correlation to global warming with the use of natural aggregates.



362 **Figure A1.** Population growth rate by year from 1960 to 2018, World Bank, 2018
 363



364 **Figure A2. a)** Natural aggregates correlated to U.S. Population Growth (USGS 1900-2006) **b)** Natural aggregates
 365 correlated to global warming (NASA 2020)
 366
 367
 368

369 **Appendix B: Albedo Model Normalization Information**

370
 371 Table 5a is reproduced from above, while Table 5b is the results of the Schneider dome area case. The results is used
 372 to demonstrate how normalization is performed
 373

374 **Table 5a.** Schneider results (Albedo=29.4118, 1950) **Table 5b.** Schneider results (Albedo=29.3654%, 2019)

Surface	Albedo	% Area of Surface	Normalized Earth Area	Weighted Albedo %
	A	B	C=A x B x (1-0.67)	A x C
Sum of Water Type		71		
Sea Ice	0.6	15	4.95	2.970
Water	0.06	56	18.48	1.109
Sum of Land Type		29		
Land - (UHI + Coverage)	0.3118	28.941	9.55053	2.978
UHI + Coverage	0.12	0.059	0.01947	0.002
		Σ=100.000	33.000	7.05882
			Cloud Area	
Clouds	0.3336	67	67	22.35294
Σ Sum Earth %			100.000	
Σ Global Albedo				29.4118

Surface	Albedo	Normalized % Surface Area	Normalized Earth Area	Weighted Albedo %
	A	B	C=A x B x (1-0.67)	A x C
Sum of Water Type		70.239		
Sea Ice	0.6	14.839	4.897	2.938
Water	0.06	55.4	18.282	1.097
Sum of Land Type		29.761		
Land - (UHI + Coverage)	0.3118	28.631	9.448	2.946
UHI + Coverage	0.12	1.1307	0.373	0.0447757
		Σ=100.000	33.000	6.980769
			Cloud Area	
Clouds	0.3336	67	67	22.3530
Σ Sum Earth %			100.000	
Σ Global Albedo				29.3786

375 Normalization is done as follows:

- 376 1. Model starts with 1950 Table 5a albedo 29.4118%, then 2019 urban coverage area is entered.
- 377 2. For example, in Table B1, the new area increases from 0.059% to 1.143%. This value is 1.084% larger,
 378 now the 'Sum of % of Earth Area' will be 101.521% in 2019.
 379

380 3. All areas are renormalized to 101.084%. For example, sea ice at 15% in 1950 becomes
 381 $15\% \times (100.000/101.084) = 14.839\%$ and the Urban Coverage becomes $1.143\% \times (100/101.521) = 1.131\%$.

382

383 **Appendix C: Related Warming Estimates and Other Amplification Factors**

384

385 Although the results obtained here at first seem to indicate that UHIs do not appear to contribute much to global
 386 warming, when the contributions of the UHI effect to the global warming feedback problem is considered, much
 387 stronger significance can be estimated. In this appendix, feedback factors are suggested providing a number of
 388 global warming estimates.

389

- 390 • *Such factors can be contentious; however, it is not uncommon to look at how factors affect each other in*
 391 *climate science. Therefore, we have chosen to provide these in this appendix mainly as an aid for the*
 392 *reader to illustrate how climate sensitivity can factor into the magnitude of UHIs warming significance.*
 393 *These estimates should be considered only as rough approximate values.*

394

395 **C.1 Global Feedback Amplification Factors**

396

397 There is a wide range of possible estimates of climate feedback sensitivity driven by uncertainties in how water
 398 vapor, clouds, and other factors change as the Earth warms. Climate feedbacks are mixed and some will amplify
 399 (positive feedback) or diminish the effect of warming from the root cause effects (for example see Hausfather 2018).
 400 The actual feedback is known to be positive (van Nes, 2015). Climatologists will often approximate such factors
 401 frequently in reference to CO₂ doubling theory as positive. For example, water-vapor feedback alone, which is one
 402 of the most important in our climate system, is thought to have the capacity to approximately double the direct
 403 warming (Manabe and Wetherald, 1967; Randall et al., 2007, Dessler et. al, 2008). This effect results from the fact
 404 that warm air holds more greenhouse moisture gas. Climate models incorporate this feedback. Water vapor feedback
 405 is strongly positive, with most evidence supporting a magnitude of 1.6 to 2.0 W/m²/K (Dessler et. al., 2008). Also
 406 water vapor feedback is considered a faster feedback mechanism (Hansen, 2008). We will use a factor of 1.75, a bit
 407 less than a doubling factor of 2. This factor would apply equally to UHI warming contribution, Greenhouse Gases
 408 (GHG), or warming due to sea ice melting.

409

410 **C.2 WAASU Model Applied to the Melting of Sea Ice**

411

412 While the Antarctic sea ice has remained roughly constant, the Arctic sea ice is melting at an alarming rate of
 413 12.85% in the last two decades (NASA sea ice, 2019). This apparent trend appears to yield an estimated 26%
 414 decrease in sea ice. It is difficult to find a strong reference for quantifying global warming impact due to Arctic sea
 415 ice melting. However, we might get an approximation using the Weighted Albedo Solar (WAS) model (and also
 416 illustrate one of the strengths of the model). Sea ice melting will result in a significant albedo change that roughly
 417 changes the ice albedo of 0.6, to the open ocean albedo of 0.06 (see Table C1 and C2). Fortunately, the Arctic areas
 418 receive only about 40% as much solar radiation (Sciencing, 2018) reducing the feedback effect. From Equation 6,
 419 the effective sea ice surface area reduction from the irradiance decrease can be approximated as

420

$$421 \text{ Effective sea ice surface area} = 15\% (1 - 0.26 \times 0.40) = 13.44\% \text{ (a 1.56\% reduction of effective area).} \quad (C-1)$$

422

423 In the WAS model, we will have to make an assumption that the effective ocean surface area increases
 424 proportionately by 1.56% to 57.56% (see Table C2). The model then finds that the global albedo change decreases
 425 from 29.4118% to 28.9948%. (Note that alternately we could have set the albedo to 29.4118% in 2019 and worked
 426 back to 1950. In this case the albedo would have increased to 29.83%).

427

428 The Global Warming (GW) is found as:

429

$$430 \%GW = \{(P/\epsilon\sigma)^{0.25}_{2019} - (P/\epsilon\sigma)^{0.25}_{1950}\} / 0.95^\circ\text{C}, \quad (C-2)$$

431

432 where $P = 340 \text{ W/m}^2 \times (1 - \text{Albedo})$ and $\epsilon = 1$. The warming increase due to ice melting is estimated from this model to
 433 be about 0.25°C or 26.4% of the 0.95°C increase in 2019. The increase in radiative forcing is 0.9452 W/m². The
 434 feedback is then roughly 1 W/m²/K where we assume a temperature change of 0.95C over this time period.

435
436
437
438
439
440
441

This figure should only be taken as a rough estimate due to numerous uncertainties as climatologists find it hard to fully quantify the seasonal variations in ice change and to know the possible impact on cloud coverage increase from additional warming evaporation. However, one would expect less evaporation in the Arctic. Thus, there are a lot of uncertainties.

Table C1. Schneider results (Albedo=29.4118, 1950) **Table C2.** Sea ice loss - albedo change (29.0643%, 2019)

Surface	Albedo	% Area of Surface	Normalized Earth Area	Weighted Albedo %
	A	B	C=A x B x (1-0.67)	A x C
Sum of Water Type		71		
Sea Ice	0.6	15	4.95	2.970
Water	0.06	56	18.48	1.109
155Sum of Land Type		29		
Land - (UHI + Coverage)	0.3118	28.941	9.55053	2.978
UHI + Coverage	0.12	0.059	0.01947	0.002
		Σ=100.000	33.000	7.05882
			Cloud Area	
Clouds	0.3336	67	67	22.35294
Σ Sum Earth %			100.000	
Σ Global Albedo				29.4118

Surface	Albedo	Normalized % Surface Area	Normalized Earth Area	Weighted Albedo %
	A	B	C=A x B x (1-0.67)	A x C
Sum of Water Type		71		
Sea Ice	0.6	13.44	4.4352	2.507
Water	0.06	57.56	18.9948	1.14
Sum of Land Type		29	23.43	
Land - (UHI + Coverage)	0.3118	28.941	9.55053	2.978
UHI + Coverage	0.12	0.059	0.01947	0.002
		100.000	33.000	6.6395
			Cloud Area	
Clouds	0.3336	67	67	22.3530
Σ Sum Earth %			123.430	
Σ Global Albedo				29.1338

442
443
444
445
446
447

C.3 Estimated Contributions to Global Warming

Table C3 summarizes the key global warming cause and effect factors that we have described.

Table C3. Global warming factors of interest

Urban Climate Amplification	Effects	Where Applied
UHI Area Amplification Factor	3.1 UHI Amplification	Applied to 2019 UHI Area
UHI Dome Horizontal Method	2.9 UHI Amplification	Applied to 2019 UHI Area
Ice Melting	0.25°C	25 °C out of 0.95 °C
Atmospheric Moisture Increase	1.75 GW Amplification	Applied to Ice Melting Temp, UHI, and GHGs +X*

448
449
450
451

where X is any other feedbacks (positive or negative)

Then major contributions to global warming can be simplified as follows for steady state warming

$$\Delta T_{GW} = \Delta T_{UHI} + \Delta T_{Water-Vapor} + \Delta T_{Sea-Ice} + \Delta T_{GHG} + \Delta T_X, \tag{C-3}$$

452
453
454
455
456
457

where $\Delta T_{GW}=0.95^\circ\text{C}$, $\Delta T_{UHI-Schneider}=0.011^\circ\text{C}$ (Table 7), $\Delta T_{Sea-Ice}=0.25^\circ\text{C}$, λ is the feedback, and ΔF is the radiative forcing change. We have three unknowns $\Delta T_{Water-Vapor}$, ΔT_{GHG} and ΔT_X . Here X is for all other feedback mechanisms like lapse rate and increases in cloud coverage and so forth, so this value can be either positive or negative. With one assumption and the following two equations we can obtain some estimates:

$$0.95^\circ\text{C} = AF_{water\ vapor}(\Delta T_{UHI} + \Delta T_{GHG}) + \Delta T_X + \Delta T_{Sea-Ice} = 1.75(0.0146^\circ\text{C} + \Delta T_{GHG}) + \Delta T_X + 0.25^\circ\text{C} \tag{C-4}$$

458
459
460
461
462

and

$$0.95^\circ\text{C} = \Delta T_{UHI} + \Delta T_{GHG+X} + \Delta T_{Sea-Ice} + \Delta T_{Water-Vapor} = 0.0147^\circ\text{C} + \Delta T_{GHG+X} + 0.25^\circ\text{C} + \Delta T_{Water-Vapor}. \tag{C-5}$$

463
464
465
466
467
468
469

To obtain some example values, we need to make an assumption since we have two equations and three unknowns. We will assume that $T_{GHG}=40\%$ of global warming so that $\Delta T_{GHG}=0.38^\circ\text{C}$. Using this estimate, with the water vapor $AF_{water-vapor}=1.75$ discussed above, and equation C-4 and C5, we can obtain examples of the other factors. This are provided in Table C3 for the UHI effect variations.

These examples illustrate the UHI effect (and urban coverage) effect to Global Warming (GW) root-causes contributions that including feedback problems could range between 2.9 to 27%.

470
471
472
473
474
475
476

From the table the UHI effective feedback contribution are 2.43 (2.87%/1.18%), 2.3 (7.32%/3.16%), 2.2 (12.5%/5.7%) , 1.8 (27.3%/15%) averaging 2.2. These values indicate that the UHI area feedback contribution could increase by 2.2 from 0.096 to about 0.21W/m²/% Normalized Effective Amplified Area (see Table 7). Although these values are crude estimates, they serve as possible helpful examples.

Table C3. Global warming contributions (2019)

Warming Component	Temperature Contribution (°C)	GW Percent Root-Cause Contribution	Percent of GW	Temperature Contribution (°C)	GW Percent Root-Cause Contribution	Percent of GW
Schneider Study						
UHI Area Amplification=3.1			UHI Dome Amplification=8.4			
Urbanization	0.0112	2.87%	1.18%	0.03002	7.32%	3.16%
Greenhouse gases (40%)	0.38	97.13%	40.0%	0.38	92.68%	40.00%
Sea ice melting feedback	0.25		26.32%	0.25		26.32%
Water vapor feedback	0.2944		31%	0.31028		32.66%
X (Other)	0.0144		1.51%	-0.0203		-2.14%
Total	∑0.95					
GRUMP Study						
UHI Area Amplification=3.1			UHI Dome Amplification=8.4			
Urbanization	0.0542	12.47%	5.70%	0.1425	27.27%	15.00%
Greenhouse gases (35%)	0.38	87.53%	40%	0.38	72.73%	40.00%
Sea ice melting feedback	0.25		26.32%	0.25		26.32%
Water vapor feedback	0.331		34.8%	0.405		42.63%
X (Other)	-0.0648		-6.82%	-0.2275		-23.95%
Total	∑0.95					

477
478
479
480
481
482**Appendix D: WAASU Model References**

Table D1 provides references for the WAASU model values.

Table D1 Key References for WAASU model

Parameter	Albedo (reference)	1950 Area (reference)
Sea Ice	50-70%, average 60% (NSID 2020)	15% (Lindsey 2019)
Water	0.06 (NSIDC 2020)	56% Ocean+Sea Ice=71% (USGS)
Land-(UHI+Coverage)	Adjusted to obtain 29.412% and surface reflected of 7.06 Earth Albedo in 1950 thereafter held fixed (see IPCC Hartmann (2013) AR5 report)	29%-Urban Coverage
UHI+Cov	0.12 Sugawara et. Al (2014)	See Table 1
Clouds	22.35294 (IPCC Hartmann et al., 2013)	67% (Earthobservatory, NASA)
Earth Albedo	29.412% (IPCC Hartmann, 2013)	-

483
484
485
486
487
488
489
490
491
492
493
494
495
496
497
498
499
500**References**

- Barr J. M., 2019 The Economics of Skyscraper Height (Part IV): Construction Costs Around the World, <https://buildingtheskyline.org/skyscraper-height-iv/>
- Basara J. ,P. Hall Jr. , A.Schroeder , B.Illston ,K.Nemunaitis 2008, Diurnal cycle of the Oklahoma City urban heat island, J. of Geophysical Research
- Cao C.X. , Zhao J., P. Gong, G. R. MA, D.M. Bao, K.Tian, Wetland changes and droughts in southwestern China, Geomatics, Natural Hazards and Risk, Oct 2011, <https://www.tandfonline.com/doi/full/10.1080/19475705.2011.588253>
- Cormack L. 2015 Where does all the stormwater go after the Sydney weather clears? The Sydney Morning Herald, <https://www.smh.com.au/environment/where-does-all-the-stormwater-go-after-the-sydney-weather-clears-20150430-1mx4ep.html>
- Dessler A. E. ,Zhang Z., Yang P., Water-vapor climate feedback inferred from climate fluctuations, 2003–2008, *Geophysical Research Letters*, (2008), <https://doi.org/10.1029/2008GL035333>
- Earthobservatory, NASA (clouds albedo 0.67) <https://earthobservatory.nasa.gov/images/85843/cloudy-earth>
- Fan, Y., Li, Y., Bejan, A. *et al.* Horizontal extent of the urban heat dome flow. *Sci Rep* 7, 11681 (2017). <https://doi.org/10.1038/s41598-017-09917-4>

- 501 Feddema, J. J., K. W. Oleson, G. B. Bonan, L. O. Mearns, L. E. Buja, G. A. Meehl, and W. M. Washington (2005),
 502 The importance of land-cover change in simulating future climates, *Science*, **310**, 1674– 1678,
 503 doi:10.1126/science.1118160
- 504 Galka M. 2016, Half the World Lives on 1% of Its Land, Mapped, [https://www.citylab.com/equity/2016/01/half-](https://www.citylab.com/equity/2016/01/half-earth-world-population-land-map/422748/)
 505 [earth-world-population-land-map/422748/](http://metrocosm.com/world-population-split-in-half-map/), , (2016 publication on 2000 data set, [http://metrocosm.com/world-](http://metrocosm.com/world-population-split-in-half-map/)
 506 [population-split-in-half-map/](http://metrocosm.com/world-population-split-in-half-map/))
- 507 Global Rural Urban Mapping Project (GRUMP) 2005, Columbia University Socioeconomic Data and Applications
 508 Center, Gridded Population of the World and the Global Rural-Urban Mapping Project (GRUMP).
- 509 Hansen, J., "2008: Tipping point: Perspective of a climatologist." Archived 2011-10-22 at the Wayback Machine,
 510 Wildlife Conservation Society/Island Press, 2008. Retrieved 2010.
- 511 Hartmann, D.L., A.M.G. Klein Tank, M. Rusticucci, L.V. Alexander, S. Brönnimann, Y. Charabi, F.J. Dentener,
 512 E.J. Dlugokencky, D.R. Easterling, A. Kaplan, B.J. Soden, P.W. Thorne, M. Wild and P.M. Zhai, 2013:
 513 Observations: Atmosphere and Surface. In: *Climate Change 2013: The Physical Science Basis. Contribution of*
 514 *Working Group I to the Fifth Assessment Report of the Intergovernmental Panel on Climate Change* [Stocker,
 515 T.F., D. Qin, G.-K. Plattner, M. Tignor, S.K. Allen, J. Boschung, A. Nauels, Y. Xia, V. Bex and P.M. Midgley
 516 (eds.)]. Cambridge University Press, Cambridge, United Kingdom and New York, NY, USA.
- 517 Hirshi M. ,Seneviratne S. , V. Alexandrov, F. Boberg, C. Boroneant, O. Christensen, H. Formayer, B. Orlowsky &
 518 P. Stepanek, Observational evidence for soil-moisture impact on hot extremes in Europe, *Nature Geoscience* **4**,
 519 17-21 (2011)
- 520 Huang Q. , Lu Y. 2015 Effect of Urban Heat Island on Climate Warming in the Yangtze River Delta Urban
 521 Agglomeration in China, *Intern. J. of Environmental Research and Public Health* **12** (8): 8773 (30%)
- 522 Jones, P. D., D. H. Lister, and Q.-X. Li, 2008: Urbanization effects in large-scale temperature records, with an
 523 emphasis on China. *J. Geophys. Res.*, **113**, D16122, doi: 10.1029/2008JD009916.
- 524 Lindsey R, Scott M., (2019), Climate Change: Arctic Sea Ice Summer Minimum, NOAA Climate.gov,
 525 <https://www.climate.gov/news-features/understanding-climate/climate-change-minimum-arctic-sea-ice-extent>
- 526 Manabe, S., and R. T. Wetherald (1967), Thermal equilibrium of atmosphere with a given distribution of relative
 527 humidity, *J. Atmos. Sci.*, **24**, 241–259.
- 528 McKittrick R. and Michaels J. 2004. A Test of Corrections for Extraneous Signals in Gridded Surface Temperature
 529 Data, *Climate Research*
- 530 McKittrick R., Michaels P. 2007 Quantifying the influence of anthropogenic surface processes and inhomogeneities
 531 on gridded global climate data, *J. of Geophysical Research-Atmospheres*
- 532 McKittrick Website Describing controversy: <https://www.rossmckittrick.com/temperature-data-quality.html>
 533 NASA 1900-2006 updated, 2020 <https://climate.nasa.gov/vital-signs/global-temperature/>
- 534 NASA 2000, Gridded population of the world, , [https://sedac.ciesin.columbia.edu/data/set/gpw-v3-population-](https://sedac.ciesin.columbia.edu/data/set/gpw-v3-population-count/data-download)
 535 [count/data-download](https://sedac.ciesin.columbia.edu/data/set/gpw-v3-population-count/data-download)
- 536 NASA Sea Ice, (2019) <https://climate.nasa.gov/vital-signs/arctic-sea-ice/>
- 537 NSID 2020, National Snow & Ice Data Center, "Thermodynamics: Albedo". nsidc.org. Retrieved 14 August 2016.
 538 <https://nsidc.org/cryosphere/seaice/processes/albedo.html>
- 539 Randall, D. A. et al. (2007), Climate models and their evaluation, in *Climate Change 2007: The Physical Science*
 540 *Basis. Contributions of Working Group I to the Fourth Assessment Report of the Intergovernmental Panel on*
 541 *Climate Change*, edited by S. Solomon et al., pp. 591–662, Cambridge Univ. Press, Cambridge, U.K.
- 542 Ren, G.; Chu, Z.; Chen, Z.; Ren, Y. **2007** Implications of temporal change in urban heat island intensity observed at
 543 Beijing and Wuhan stations. *Geophys. Res. Lett.* , **34**, L05711,doi:10.1029/2006GL027927.
- 544 Ren, G.-Y., Z.-Y. Chu, J.-X. Zhou, et al., (2008): Urbanization effects on observed surface air temperature in North
 545 China. *J. Climate*, **21**, 1333-1348
- 546 Schmidt G. A. 2009 Spurious correlations between recent warming and indices of local economic activity, *Int. J. of*
 547 *Climatology*
- 548 Schneider, A., M. Friedl, and D. Potere, 2009: A new map of global urban extent from MODIS satellite data.
 549 *Environmental Research Letters*, **4**(4), 044003, doi:10.1088/1748-9326/4/4/044003
- 550 Satterthwaite D.E., F. Aragón-Durand, J. Corfee-Morlot, R.B.R. Kiunsi, M. Pelling, D.C. Roberts, and W. Solecki,
 551 2014: Urban areas. In: *Climate Change 2014: Impacts, Adaptation, and Vulnerability. Part A: Global and*
 552 *Sectoral Aspects. Contribution of Working Group II to the Fifth Assessment Report of the Intergovernmental*
 553 *Panel on Climate Change (IPCC)*
- 554 Sciencing (2018) <https://sciencing.com/sun-intensity-vs-angle-23529.html>
- 555 Stone B. 2009 Land use as climate change mitigation, *Environ. Sci. Technol.*, **43**(24), 9052– 9056,
 556 doi:10.1021/es902150g
- 557 Sugawara, H., Takamura, T. Surface Albedo in Cities (0.12): Case Study in Sapporo and Tokyo, Japan. *Boundary-*
 558 *Layer Meteorol* **153**, 539–553 (2014). <https://doi.org/10.1007/s10546-014-9952-0>
- 559 US Population Growth 1900-2006, u-s-history.com/pages/h980.html
- 560 USGS 1900-2006, Materials in Use in U.S. Interstate Highways, <https://pubs.usgs.gov/fs/2006/3127/2006-3127.pdf>
- 561 USGS on Amount of Earth covered by water, [https://www.usgs.gov/special-topic/water-science-](https://www.usgs.gov/special-topic/water-science-school/science/how-much-water-there-earth?qt-science_center_objects=0#qt-science_center_objects)
 562 [school/science/how-much-water-there-earth?qt-science_center_objects=0#qt-science_center_objects](https://www.usgs.gov/special-topic/water-science-school/science/how-much-water-there-earth?qt-science_center_objects=0#qt-science_center_objects)

563 van Nes E. H., Scheffer M., Brovkin V., Lenton T. M., Ye H, Deyle E. and Sugihara G., Nature Climate Change
564 2015. dx.doi.org/10.1038/nclimate2568
565 World Bank, 2018 population growth rate, worldbank.org
566 Yang, X.; Hou, Y.; Chen, B. 2011 Observed surface warming induced by urbanization in east China. *J. Geophys.*
567 *Res. Atmos*, 116, doi:10.1029/2010JD015452.
568 Zhang, X., Friedl, M. A., Schaaf, C. B., Strahler, A. H. & Schneider, A. 2004 The footprint of urban climates on
569 vegetation phenology. *Geophys. Res. Lett.* 31, L12209
570 Zhao, Z.-C., 1991: Temperature change in China for the last 39 years and urban effects. *Meteorological Monthly* (in
571 Chinese), 17(4), 14-17.
572 Zhao, Z.-C., 2011: Impacts of urbanization on climate change. in: 10,000 Scientific Difficult Problems: Earth
573 Science, 10,000 scientific difficult problems Earth Science Committee Eds., Science Press, 843-846. 30%
574 Zhao L, Lee X, Smith RB, Oleson K, Strong 2014, contributions of local background climate to urban heat islands,
575 *Nature*. 10;511(7508):216-9. doi: 10.1038/nature13462
576 Zhou D. , Zhao S. , L. Zhang, G Sun and Y. Liu, 2015, The footprint of urban heat island effect in China, *Scientific*
577 *Reports*. 5: 11160
578 Zhou Y. , SmithS. , Zhao K. , M. Imhoff, A. Thomson, B. Lamberty,G. Asrar, X. Zhang, C. He and C. Elvidge, A
579 global map of urban extent from nightlights, *Env. Research Letters*, 10 (2015), (study uses a 2000 data set).
580
581
582
583 **Conflicts of Interest**
584 The author declares that he has no conflicts of interest.
585